Supporting information

Highlighting the Role of the Random Associating Block in the Self-Assembly of Amphiphilic Block-Random Copolymers

*Lionel Lauber, Christophe Chassenieux, Taco Nicolai and Olivier Colombani**

1) Synthesis

The synthesis of MH50 and DH50 by ATRP was already described[1-2]. The synthesis of the other P(nBA$_{(1-x)}$-*stat*-AA$_x$)$_{100}$ (MHx) and P(nBA$_{(1-x)}$-*stat*-AA$_x$)$_{100}$-*b*-PAA$_{100}$ (DHx), where x stands for the percentage of acrylic acid units in the hydrophobic block, was adapted from that of MH50 and DH50.

Briefly, methyl 2-bromopropionate (MBP), a monofunctional initiator, was used to prepare a monofunctional macroinitiator poly(n-butyl acrylate$_{(1-x)}$–*stat*–*tert*-butyl acrylate$_x$)$_{100}$−Br, P(nBA$_{(1-x)}$−*stat*−tBA$_x$)$_{100}$−Br. N,N,N′,N″-pentamethyldiethylenetriamine (PMDETA)/CuBr was used as catalyst in the following proportions: [nBA]:[tBA]:[MBP]:[CuBr]:[CuBr$_2$]:[PMDETA] = 100*(1-x):100*x:1:0.7:0.035:0.74. Anisole (monomers/anisole = 90/10 g/g) was used both as solvent and as internal standard to determine the monomer conversion by gas chromatography during the polymerization.[3-4] The polymerization was allowed to proceed at 60°C until a conversion of 50%. The reaction was then stopped and the polymer was purified by column chromatography (silica/$CHCl_3$)

followed by precipitation into methanol/water (90/10 vol/vol). Size exclusion chromatography (SEC) and ^{1}H NMR were used to characterise the polymer confirming its chemical structure as shown in Table S1.

To produce a P(nBA$_{(1-x)}$−*stat*−tBA$_x$)$_{100}$−*b*−PAA$_{100}$−Br diblock copolymer, the aforementioned macroinitiator P(nBA$_{(1-x)}$−*stat*−tBA$_x$)$_{100}$−Br was used to initiate the polymerisation of *tert*-butyl acrylate using the following proportions of reagents: [tBA]:[macroinitiator]:[CuBr]:[CuBr$_2$]:[PMDETA] = 200:1:0.7:0.035:0.74 and a monomer/anisole ratio of 90/10 g/g. After polymerization at 60°C, the reaction was again stopped at 50% conversion and purification was achieved as for the first block. The final step used trifluoroacetic acid to selectively and quantitatively transform the *tert*-butyl acrylate units into acrylic acid units by acidolysis.[5] The MHx and DHx were obtained by respectively acidolysing the corresponding P(nBA$_{(1-x)}$−*stat*−tBA$_x$)$_{100}$−Br macroinitiator or the P(nBA$_{(1-x)}$−*stat*−tBA$_x$)$_{100}$−*b*−PAA$_{100}$−Br diblock. After acidolysis, purification was done by precipitation into pentane. The final polymers were characterized by ^{1}H, ^{13}C NMR and by titration, confirming quantitative and selective acidolysis.

^{1}H, ^{13}C NMR spectra were recorded at 20 °C on a Brüker AC400 (400 MHz) spectrometer using $CDCl_3$, MeOD or THF-D_8.

Size exclusion chromatography analysis was done with an equipment consisting of a guard column (5 µm, 50 mm × 7.5 mm) connected to a PLgel Mixed-D column (5 µm, 300 mm ×7.5 mm) and a PLgel "individual pore size" column (5 µm, 50 mm ×7.5 mm) operating at room temperature in THF with a flow rate of 1 mL.min^{-1}. After filtration through a 0.2 µm pore size membrane, injection was done at a polymer concentration of ~5 mg.mL^{-1} in THF. In all cases except DH50 which had been synthesized and analyzed previously, absolute average molar masses were calculated using a light scattering (miniDAWN TREOS from Wyatt) and an

Online refractive index (RID10A from Shimadzu) detectors with a specific refractive index increment of the polymer in THF of 0.057 mL/g.[3] For the precursor of DH50, molecular weights were determined as PS-equivalents using PS-standards for calibration of the SEC.

Table S1. Characteristics of the copolymers synthesized. [a] Theoretical M_n calculated from the conversion. [b] Theoretical M_n calculated assuming 100% acidolysis.

	Before acidolysis			After acidolysis
Name	$M_{n,theo}$ (g/mol)[a]	$M_{n,SEC}$ (g/mol)	Đ	$M_{n,theo}$ (g/mol)[b]
MH40	1.22 x10^4	1.25 x10^4	1.17	1.00 x10^4
MH50[c]	1.28 x10^4	1.25 x10^4	1.10	1.00 x10^4
MH60	1.26 x10^4	1.36 x10^4	1.34	1.03 x10^4
DH40	2.55 x10^4	2.52 x10^4	1.17	1.74 x10^4
DH50	2.54 x10^4	2.56 x10^4	1.10	1.72 x10^4
DH60	2.50 x10^4	2.72 x10^4	1.13	1.59 x10^4

2) Phase separation

Figure S1, Figure S2 and Figure S3 represent the dependences of M_w on the concentration of Na^+ at several ionization degrees at C=2 g/L, for MH50, MH40 and MH60, respectively. It appears that adding salt has two effects on MHx. It causes an increase of the aggregation number at a given ionization degree and decreases the solubility of the polymer. For MH50, the aggregation number increases with increasing [Na^+] at α=0.5 and 0.7 until precipitation. However, at α=1 unimers are present at all [Na^+] until the system phase separates for [Na^+]>1.5 M.

There is a threshold value of [Na^+] for each ionization degree at which the polymer precipitated, characterized by clouding of the solutions. This critical value is represented as dashed lines and it decreases with the decrease of α. Phase separation leads to the formation of a viscous bottom phase containing most of the polymer. Light scattering measurements showed that the top phase contained a small amount of polymer at least just above the critical value (data not shown).

The salt induced phase separation occurred at different ionization degrees depending on x. The phase diagram of MHx as a function of [Na^+] and the ionization degree is shown in Figure S4a. As might be expected a decrease in the fraction of AA units x favours phase separation.

The phase diagram of the MHx as a function of [Na^+] and the fraction of charged units is shown in Figure S4b. Good correlation is found between [Na^+] and the fraction of charged units for the three copolymers, demonstrating that the solubility of MHx is principally controlled by the charge density. The maximum fraction of charged units (f_{MHx}) when α=1 is indicated by dashed lines on Figure S4b.

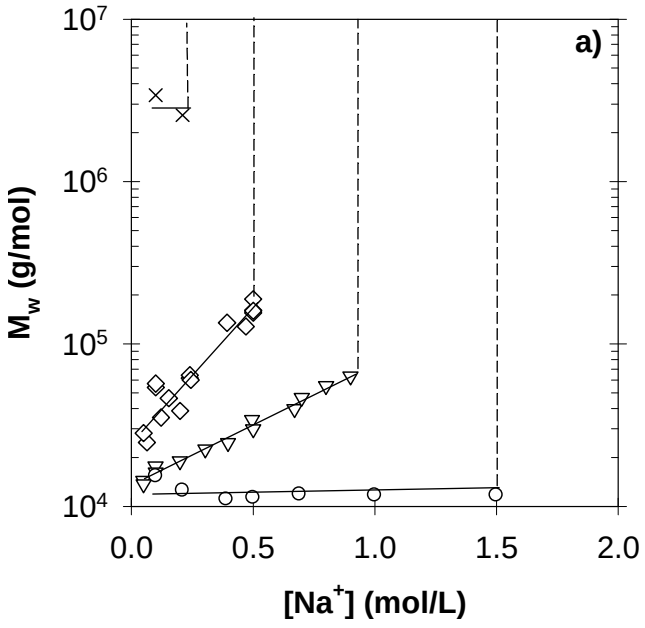

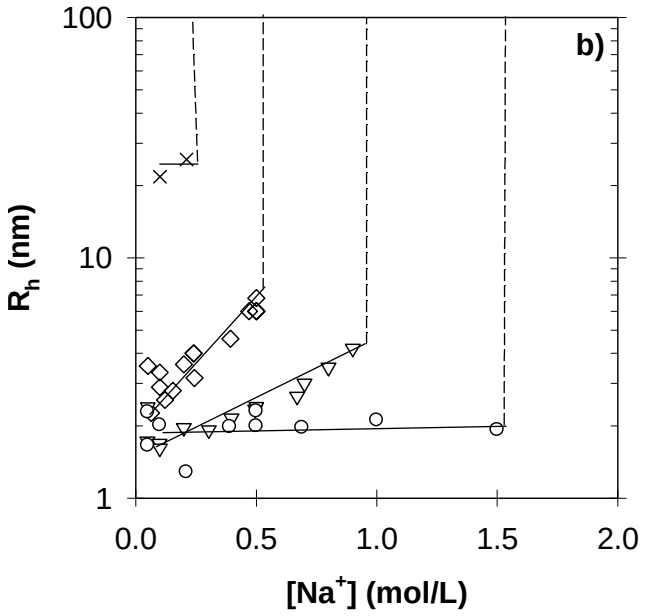

Figure S1. Molar mass M_w (a) and hydrodynamic radius R_h (b) as a function of the concentration of Na^+ for MH50 at 2 g/L and α=1 (○), 0.7 (▽), 0.5 (◇) and 0.3 (×). The solid lines are guides to the eye. The vertical dashed lines indicate the onset of phase separation.

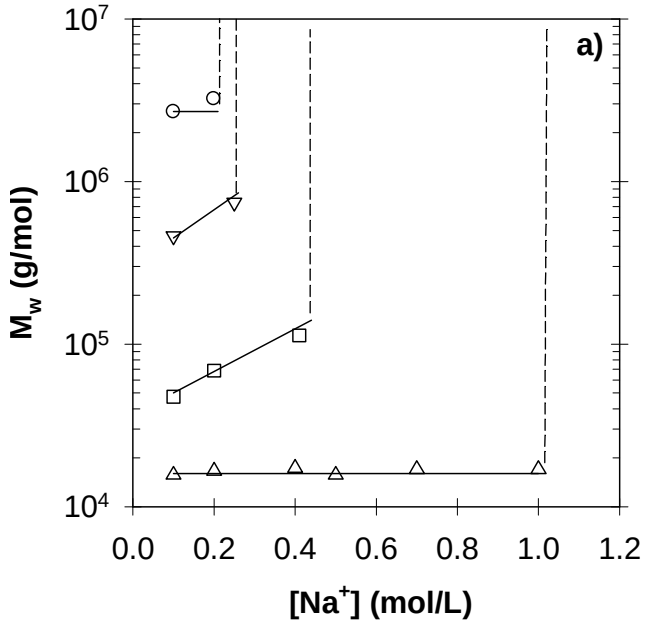

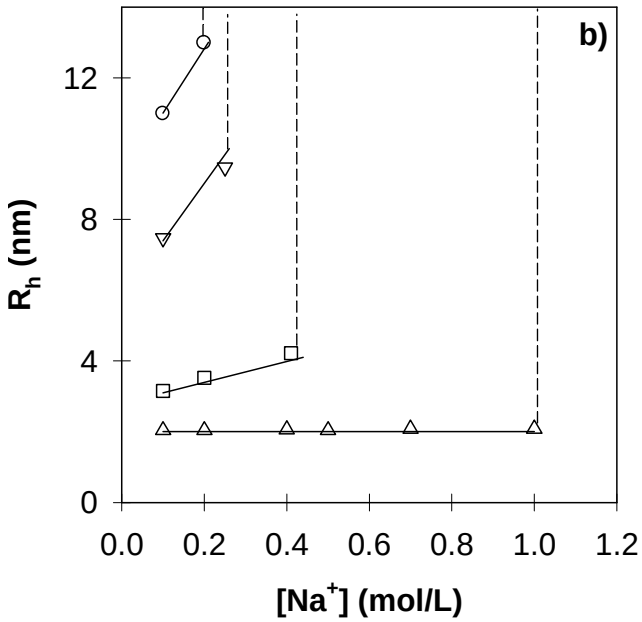

Figure S2. Molar mass M_w (a) and hydrodynamic radius R_h (b) as a function of the concentration of Na^+ for MH40 at 2 g/L and α=1 (Δ), 0.7 (□), 0.5 (∇), 0.35 (○).The solid lines are guides to the eye. The vertical dashed lines indicate the onset of phase separation.

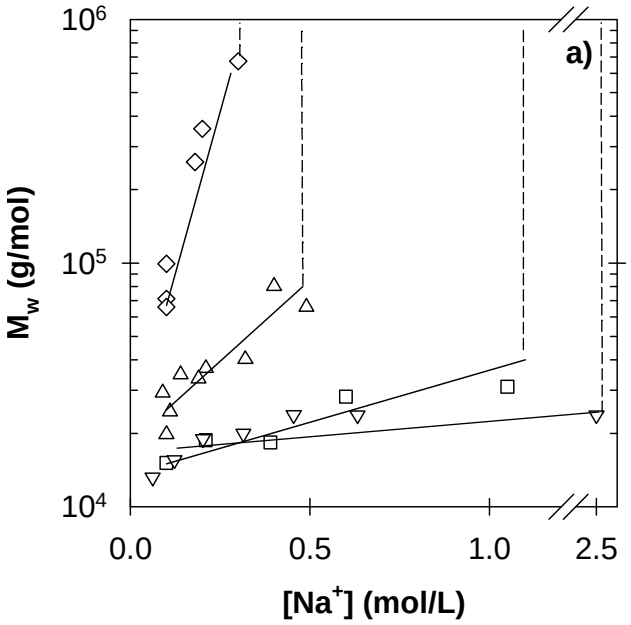

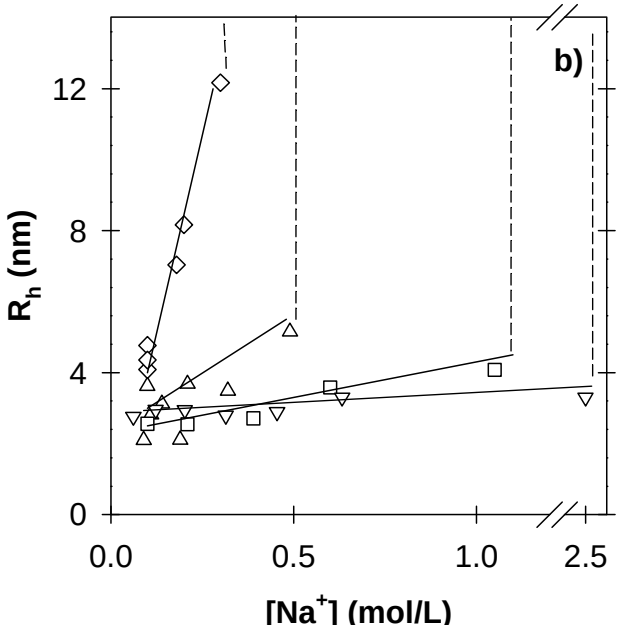

Figure S3. Molar mass M_w (a) and hydrodynamic radius R_h (b) as a function of the concentration of Na^+ for MH60 at 2 g/L and α=1 (∇), 0.7 (□), 0.5 (Δ), 0.2 (◇). The solid lines are guides to the eye. The vertical dashed lines indicate the onset of phase separation.

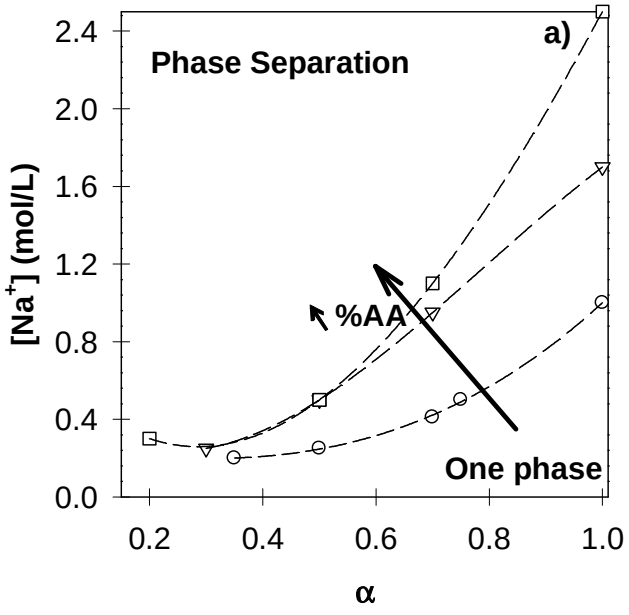

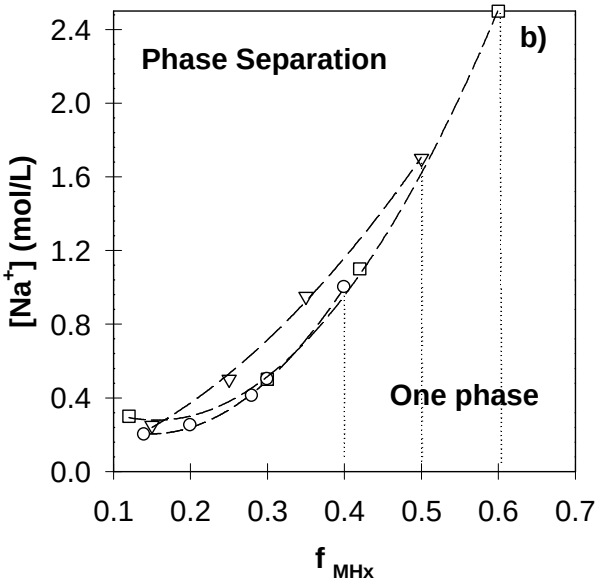

Figure S4. Phase diagram of MH40 (○) MH50 (∇) and MH60 (□) at different salt concentrations as a function of the ionization degree (a) or of the fraction of charged units (b). The dashed lines are guides to the eye. The arrow in a) represents the increase of x, the AA content. The vertical dotted lines in b) correspond to the fraction of charged units within the MHx blocks for $\alpha = 1$.

3) Influence of the concentration

As explained in the "Material and Methods" section of the paper, the effects of the concentration were systematically checked in order to choose a suitable concentration to measure M_w. For all the copolymers, 2 g/L of copolymer is an appropriate polymer concentration where interactions between the scatterers can be neglected.

i. MH40

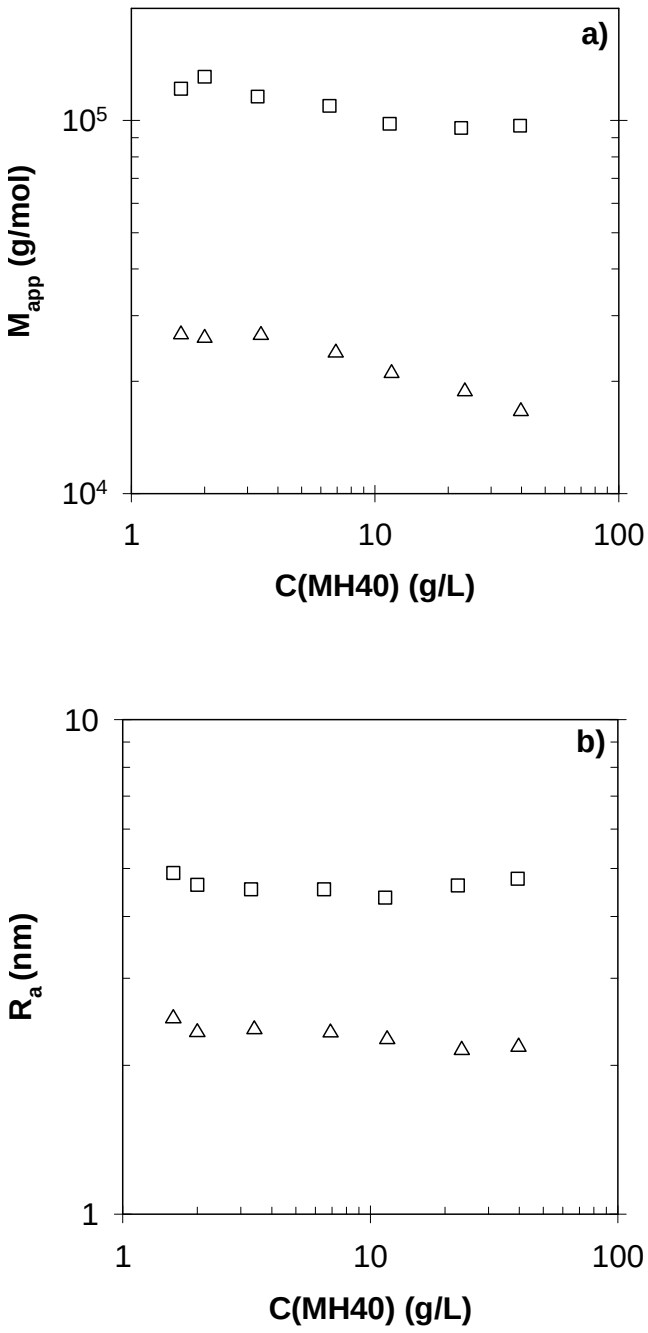

Figure S5. Apparent molar mass M_{app} (a) and apparent hydrodynamic radius R_a (b) as a function of the concentration of MH40 at $[Na^+]$=0.1M and at α=0.6 (□) and 0.78 (Δ).

ii. MH60

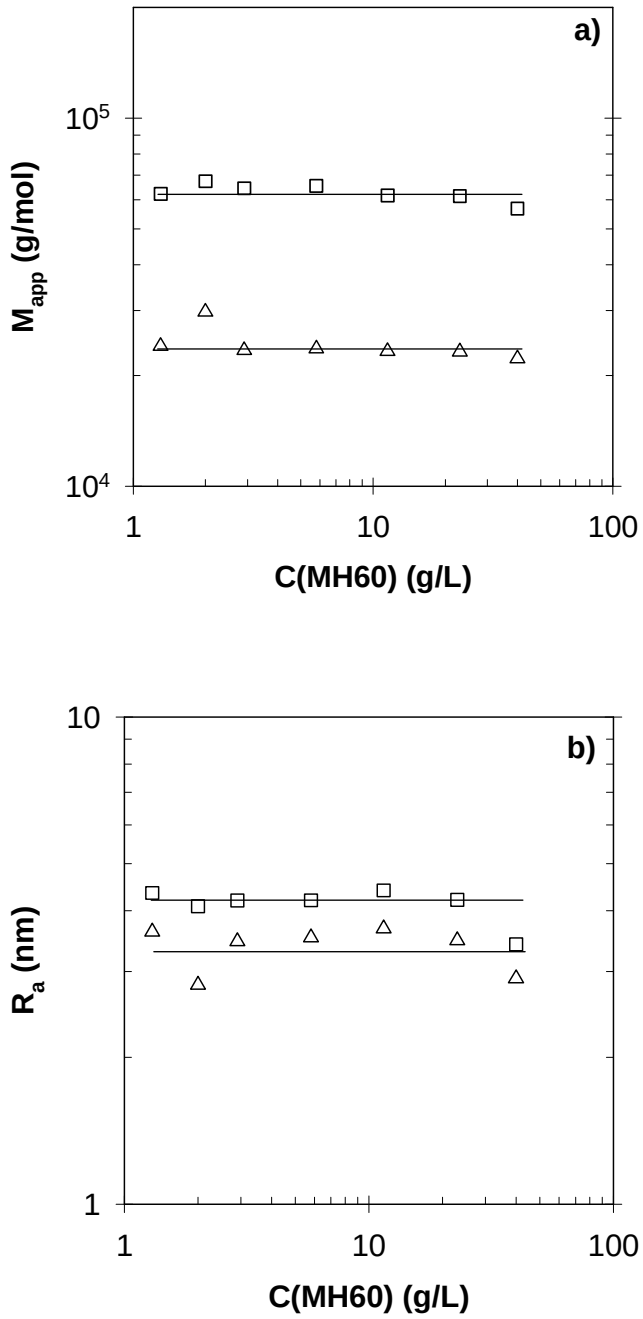

Figure S6. Apparent molar mass M_{app} (a) and apparent hydrodynamic radius R_a (b) as a function of the concentration of MH60 at $[Na^+]$=0.1M and at α=0.23 (□) and 0.49 (Δ). The solid lines are guides to the eye.

iii. DH40

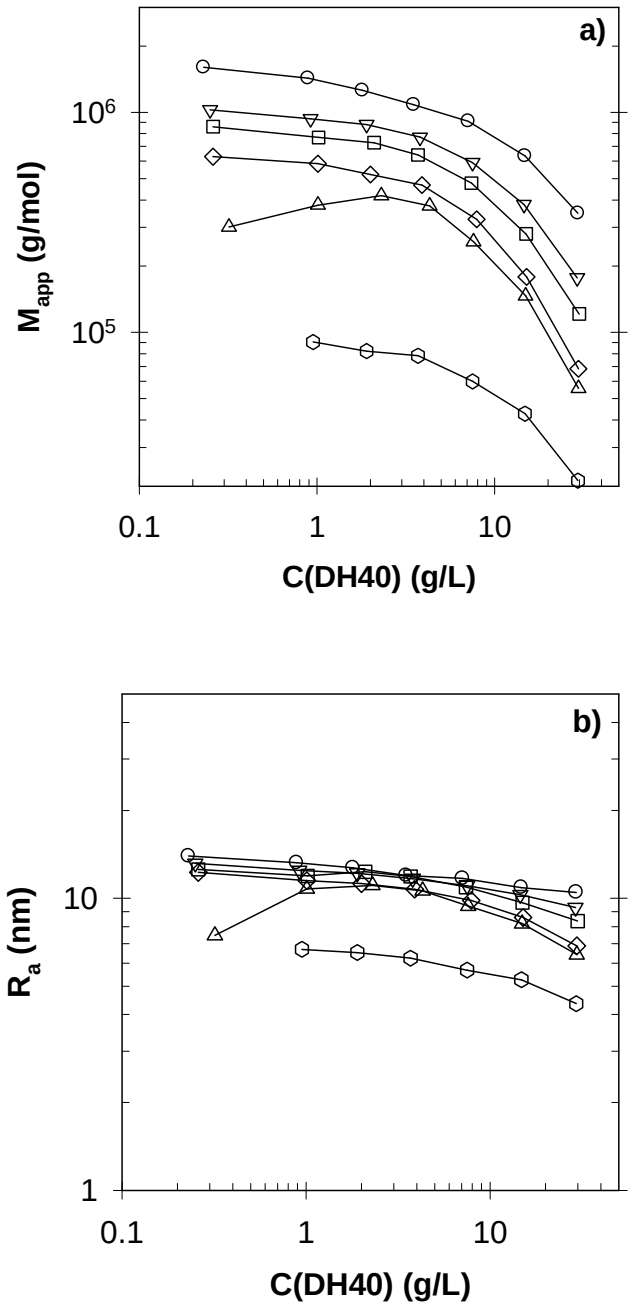

Figure S7. Apparent molar mass M_{app} (a) and apparent hydrodynamic radius R_a (b) as a function of the concentration of DH40 at $[Na^+]$=0.5M and at α=0.24 (○), 0.34 (▽), 0.42 (□), 0.53 (◇), 0.63 (△) and 0.79 (⬡). The solid lines are guides to the eye.

iv. DH60

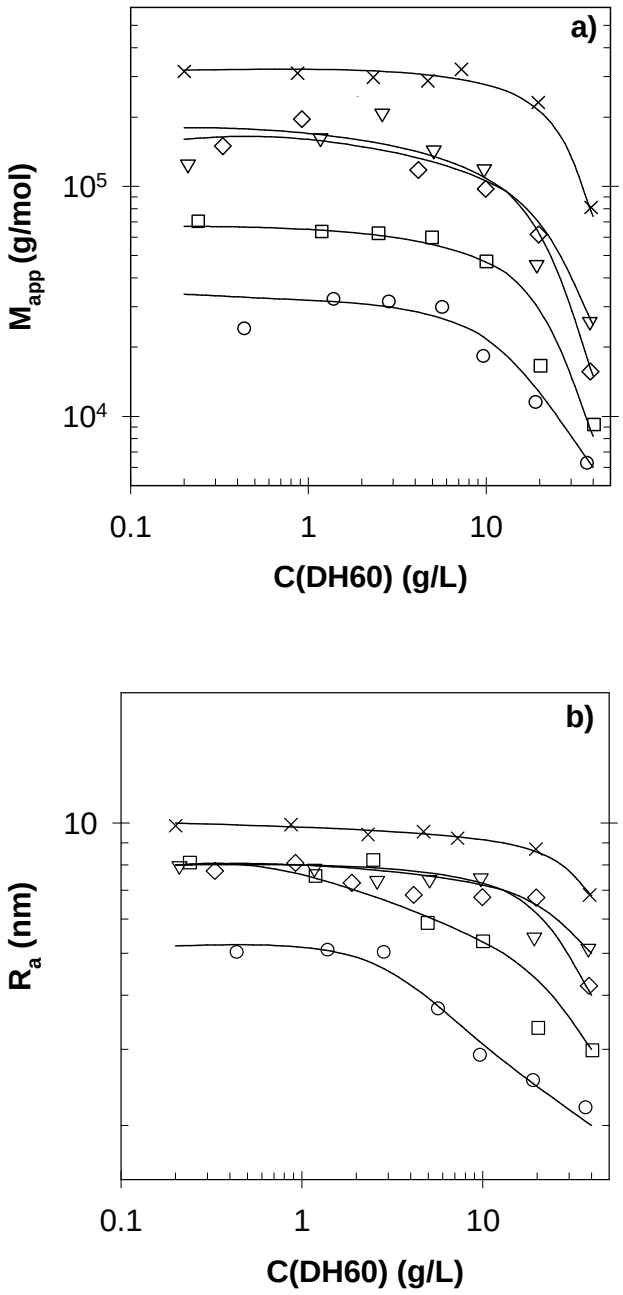

Figure S8. Apparent molar mass M_{app} (a) and apparent hydrodynamic radius R_a (b) as a function of the concentration of DH60 at $[Na^+]$=0.5M and at α=0.09 (x), 0.23 (◊), 0.27 (∇), 0.43 (□) and 0.77 (○). The solid lines are guides to the eye.

4) Titration

For all P(nBA$_{(1-x)}$-*stat*-AA$_x$)$_{100}$ (MHx) and P(nBA$_{(1-x)}$-*stat*-AA$_x$)$_{100}$-*b*-PAA$_{100}$ (DHx) copolymers, all AA units eventually become ionized at pH > 9. However, due to differences of pK_a between the AA units in the hydrophilic corona PAA$_{100}$ and in the associating block P(nBA$_{(1-x)}$-*stat*-AA$_x$)$_{100}$, preferential ionization of the AA units within the corona occurred as depicted on Figure S9. In other words, for a given overall ionization degree of the diblock, corresponding to the average ionization degree of all AA units within the polymer, the ionization degree is lower for the AA units in the P(nBA$_{(1-x)}$-*stat*-AA$_x$)$_{100}$ block than for those in the PAA$_{100}$ block as depicted in Figure S9. Note that the experimental data represented on Figure S9 have been obtained according to an already published procedure[7] and are in good agreement with extrapolations calculated in a previous article.[3]

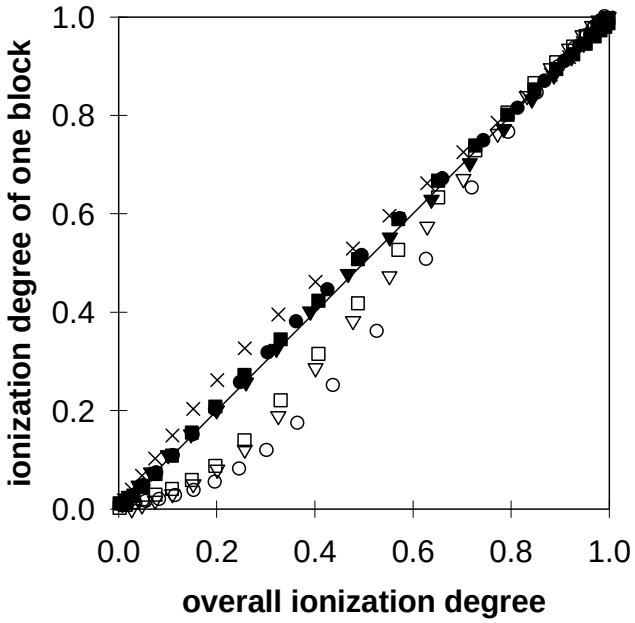

Figure S9. Degree of ionization of the AA units in the hydrophilic block PAA (×) and in the hydrophobic blocks (MH40: ○, MH50: ∇, MH60: □) as a function of the overall

ionization degree of the AA units in the diblocks (DH40: ●, DH50: ▼, DH60: ■). [Na^+]=0.1 mol/L and [AA]=0.043 mol/L. The solid lines are guides to the eye.

REFERENCES

1. E. Lejeune; M. Drechsler; J. Jestin; A. H. E. Muller; C. Chassenieux; O. Colombani. *Macromolecules* **2010,** 43, (6), 2667-2671.

2. C. Charbonneau; C. Chassenieux; O. Colombani; T. Nicolai. *Macromolecules* **2011,** 44, (11), 4487-4495.

3. A. Shedge; O. Colombani; T. Nicolai; C. Chassenieux. *Macromolecules* **2013,** 47, (7), 2439-2444.

4. O. Colombani; O. l. Langelier; E. Martwong; P. Castignolles. *J. Chem. Educ.* **2011,** 88, (1), 116-121.

5. O. Colombani; M. Ruppel; M. Burkhardt; M. Drechsler; M. Schumacher; M. Gradzielski; R. Schweins; A. H. E. Müller. *Macromolecules* **2007,** 40, (12), 4351-4362.

6. J. L. Finney; D. T. Bowron. *Curr. Opinion Coll. Interface Sci.* **2004,** 9, (1-2), 59-63.

7. O. Colombani; E. Lejeune; C. Charbonneau; C. Chassenieux; T. Nicolai. *J. Phys. Chem. B* **2012,** 116, (25), 7560-7565.